

Chapter 3

POTENTIAL-WELL DISTORTION

3.1 Static Solution

The wake potential affects the particle bunch in two ways. Static perturbation changes the shape of the bunch, while time-dependent perturbation can lead to instability of the bunch. This is analogous to quantum mechanics, where time-independent perturbation shifts the energy levels while time-dependent perturbation causes transition. In this chapter, we are going to study stationary bunch distributions, or distributions influenced by the time-independent perturbation of the wake potential. This alteration of bunch distribution is called *potential-well distortion*.

From the Vlasov equation depicted in Eq. (2.21), it is evident that the solution for the stationary particle distribution $\psi(\tau, \Delta E)$ in the longitudinal phase space must satisfy

$$[\psi, H] = 0 , \quad (3.1)$$

or it is sufficient that ψ is a function of the Hamiltonian,

$$\psi = \psi(H) . \quad (3.2)$$

Recall that the Hamiltonian of a particle with small amplitude synchrotron oscillations is

$$H = -\frac{\eta}{2v\beta^2 E_0}(\Delta E)^2 - \frac{\omega_{s0}^2 \beta^2 E_0}{2\eta v} \tau^2 + V(\tau) , \quad (3.3)$$

which describes the motion of a beam particle in the potential well

$$U(\tau) = -\frac{\omega_{s0}^2 \beta^2 E_0}{2\eta v} \tau^2 + V(\tau) , \quad (3.4)$$

where ΔE and τ are the energy offset and time advance of the beam particle, while the synchronous particle has energy E_0 , velocity* $v = \beta c$, bare synchrotron angular frequency ω_{s0} , and slip factor η . Here, the potential-well contributed by the wake function is [Eqs. (2.7), (2.12), and (2.18)],

$$V(\tau) = \frac{e^2}{C_0} \int_0^\tau d\tau'' \int_{\tau''}^\infty d\tau' \rho(\tau') W'_0(\tau' - \tau'') , \quad (3.5)$$

where C_0 is the length of the designed closed orbit, W'_0 is the longitudinal monopole wake function, and $\rho(\tau)$ is the linear particle density under the influence of the wake. When the effects of the wake potential is removed, this is just a parabolic potential well. In the presence of the wake potential, the potential well is distorted and the distribution of the beam particle in the longitudinal phase space is therefore modified. As will be seen below, a purely reactive wake potential, meaning that the coupling impedance is either inductive or capacitive, will modify the parabolic potential in such a way that the potential well remains symmetric. Correspondingly, the distorted particle distribution will also be head-tail symmetric, assuming that the original particle distribution in the rf potential along is symmetric. A wake potential with a resistive component, however, will affect the symmetry of the parabolic potential well so that the bunch distribution will no longer be head-tail symmetric.

3.2 Reactive Force

Consider a particle beam with linear density $\rho(s, t)$ traveling in the positive s direction with velocity v inside a cylindrical beam pipe of radius b with infinitely-conducting walls. The axis of the beam coincides with the axis of the beam pipe. The beam is assumed to be rigid; therefore $\rho = \rho(s - vt)$. We also assume at this moment that the beam is uniformly distributed transversely within a radius a which does not vary longitudinally. We are interested in the longitudinal electric field E_s seen by the beam particles at the axis of the beam. To compute that we invoke Faraday's law,

$$\vec{\nabla} \times \vec{E} = -\frac{\partial}{\partial t} \vec{B} , \quad (3.6)$$

*Here, we drop the subscript "0" for v and β for the sake of convenience.

or in the integral form,

$$\oint \vec{E} \cdot d\vec{\ell} = -\frac{\partial}{\partial t} \oint \vec{B} \cdot d\vec{A}. \quad (3.7)$$

In above, the closed path of integration of the electric field \vec{E} is along two radii of the beam pipe at s and $s + ds$ together with two length elements at the beam axis and the wall of the beam pipe, as illustrated in Fig. 3.1. The area of integration of the magnetic

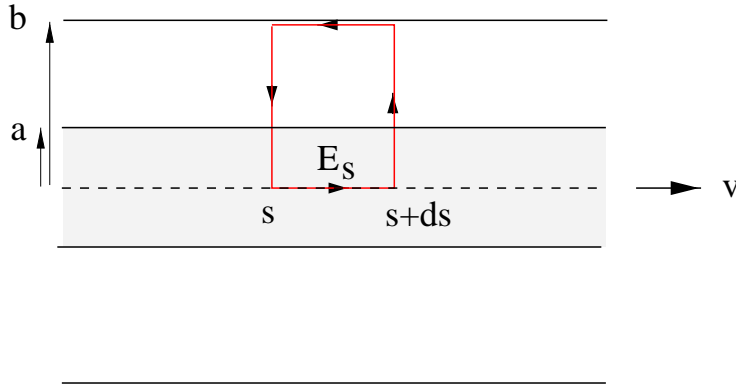


Figure 3.1: (color) Derivation of the space charge longitudinal electric field E_s experienced by a beam particle in a beam of radius a in an infinitely conducting beam pipe of radius b .

flux density \vec{B} is the area enclosed by the closed path. Now, the left side of Eq. (3.7) becomes

$$\text{L. S.} = E_s ds + \frac{e\rho(s+ds-vt)}{2\pi\epsilon_0} \left[\int_0^a \frac{rdr}{a^2} + \int_a^b \frac{dr}{r} \right] - \frac{e\rho(s-vt)}{2\pi\epsilon_0} \left[\int_0^a \frac{rdr}{a^2} + \int_a^b \frac{dr}{r} \right], \quad (3.8)$$

while the right side

$$\text{R. S.} = -\frac{\partial}{\partial t} \frac{\mu_0 e\rho(s-vt)v}{2\pi} \left[\int_0^a \frac{rdr}{a^2} + \int_a^b \frac{dr}{r} \right] ds. \quad (3.9)$$

Assumption has been made that the open angle $1/\gamma$ of the radial electric field is small compared with the distance ℓ over which the linear density changes appreciably, or $b/\gamma \ll \ell$. Here, $\gamma = E_0/(mc^2)$ and m is the rest mass of the beam particle. In terms of the the squared-bracketed expressions in Eqs. (3.8) and (3.9), we can define

$$g_0 = 2 \left[\int_0^a \frac{rdr}{a^2} + \int_a^b \frac{dr}{r} \right] = 1 + 2 \ln \frac{b}{a}, \quad (3.10)$$

which is a geometric factor depending on the geometry of the beam and the beam pipe, and it will deviate from Eq. (3.10) if we relax, for example, the restriction of the transverse uniformity of the particle distribution. Combining the above, we arrive at

$$E_s + \frac{eg_0}{4\pi\epsilon_0} \frac{\partial\rho}{\partial s} = v^2 \frac{e\mu_0 g_0}{4\pi} \frac{\partial\rho}{\partial s}, \quad (3.11)$$

or

$$E_s = -\frac{eg_0}{4\pi\epsilon_0\gamma^2} \frac{\partial\rho}{\partial s}, \quad (3.12)$$

which is the space charge force experienced by a particle in a beam. In the reduction from Eq. (3.10) to Eq. (3.12), use has been made of the relation $\epsilon_0\mu_0 = c^{-2}$.

The first application is a longitudinal harmonic wave

$$\rho_1(s, t) \propto e^{i(ns/R - \Omega t)}, \quad (3.13)$$

perturbing a coasting beam of uniform linear density ρ_0 , where n is a revolution harmonic, R is the radius of the accelerator ring, and Ω is the frequency of the wave. It will be shown in Chapter 6 that $\Omega \approx n\omega_0 = nv/R$; the difference comes from the perturbation of the coupling impedance. Thus, ρ_1 is roughly a function of $s - vt$. Substitution into Eq. (3.12) results in the voltage

$$V = -E_s C_0 = \frac{ineZ_0cg_0}{2\gamma^2} \rho_1 \quad (3.14)$$

seen by a beam particle per accelerator turn. The perturbing wave constitutes a perturbing current $I_1 = e\rho_1 v$. Therefore, the space charge impedance per harmonic seen is

$$\left. \frac{Z_0^{\parallel}}{n} \right|_{\text{sp ch}} = \frac{iZ_0g_0}{2\gamma^2\beta}, \quad (3.15)$$

which is to be compared with Eq. (1.36). From Eq. (3.12), the space charge force experienced by a beam particle at position s and time t becomes

$$F(s, t) = \frac{ie^2v}{2\pi} \left. \frac{Z_0^{\parallel}}{n} \right|_{\text{sp ch}} \frac{\partial\rho(s, t)}{\partial s}. \quad (3.16)$$

Since an inductive impedance can be viewed as a negative space charge impedance, we can write the force due to a general reactive impedance as

$$F(s, t) = \frac{ie^2v}{2\pi} \left. \frac{Z_0^{\parallel}}{n} \right|_{\text{reactive}} \frac{\partial\rho(s, t)}{\partial s}. \quad (3.17)$$

When the position of the beam particle is measured in terms of time advanced τ ahead of the synchronous particle, the particle linear distribution $\lambda(\tau, t)$, which is normalized to the total number of beam particles, is related to $\rho(s, t)$ by

$$\rho(s, t)ds = \lambda(\tau, t)d\tau \quad \text{or} \quad \frac{\partial \rho(s, t)}{\partial s} = \frac{1}{v^2} \frac{\partial \lambda(\tau, t)}{\partial \tau} . \quad (3.18)$$

The reactive force exerted on a beam particle becomes

$$F(\tau, t) = \frac{ie^2}{2\pi v} \frac{Z_0^{\parallel}}{n} \Bigg|_{\text{reactive}} \frac{\partial \lambda(\tau, t)}{\partial \tau} . \quad (3.19)$$

Of course, the above expression can also be obtained by substituting the reactive wake function

$$W_0'(\tau) = \delta'(\tau) \left[\frac{i}{\omega_0} \frac{Z_0^{\parallel}}{n} \right]_{\text{reactive}} \quad (3.20)$$

directly into Eq. (2.7).

The second application is on potential-well distortion. For a bunch, the head has a negative slope or $\partial \lambda / \partial \tau < 0$, while the tail has a positive slope or $\partial \lambda / \partial \tau > 0$. For a space charge impedance, the head of the bunch is therefore accelerated and gains energy, while the tail decelerated and loses energy. Below transition, the head arrives earlier after one turn while the tail arrives later, resulting in the spreading out of the bunch. The space charge force therefore distorts the rf potential by counteracting the rf focusing force. On the other hand, an inductive force enhances the rf focusing. The opposite is true above transition.

3.3 Haissinski Equation

For an electron bunch, because of the random quantum radiation and excitation, the stationary distribution should have a Gaussian distribution in ΔE , or

$$\psi(\tau, \Delta E) = \frac{1}{\sqrt{2\pi}\sigma_E} \exp\left(-\frac{\Delta E^2}{2\sigma_E^2}\right) \rho(\tau) , \quad (3.21)$$

where σ_E is the rms beam energy spread determined by synchrotron radiation. Noting Eq. (3.2) and the Hamiltonian in Eq. (3.3), we must have

$$\psi(\tau, \Delta E) \propto \exp\left(\frac{v\beta^2 E_0}{\eta\sigma_E^2} H\right) . \quad (3.22)$$

The linear density or distribution $\rho(\tau)$ is obtained by an integration over ΔE . Since Hamiltonian H depends on $\rho(\tau)$ [see, for example, Eqs. (2.19) and (2.20)], we finally arrive at a self-consistent equation for the linear density,

$$\rho(\tau) = \rho(0) \exp \left[- \left(\frac{\omega_{s0} \beta^2 E_0}{\eta \sigma_E} \right)^2 \frac{\tau^2}{2} + \frac{e^2 \beta^2 E_0}{\eta T_0 \sigma_E^2} \int_0^\tau d\tau'' \int_{\tau''}^\infty d\tau' \rho(\tau') W_0'(\tau' - \tau'') \right]. \quad (3.23)$$

This is called the *Haissinski equation* [1], where the constant $\rho(0)$ is obtained by normalizing to the total number of particles in the bunch:

$$\int d\tau \rho(\tau) = N. \quad (3.24)$$

The solution will give a linear distribution that deviates from the Gaussian form, and we call this *potential-well distortion*. Since the rf voltage is modified, the angular synchrotron frequency also changes from ω_{s0} to the perturbed incoherent ω_s accordingly.

For a purely resistive impedance $Z_0^{\parallel}(\omega) = R_s$ with the wake function $W_0'(z) = R_s \delta(z/v)$, the equation can be solved analytically giving the solution [3]

$$\rho(\tau) = \frac{\sqrt{2/\pi} e^{-\tau^2/(2\sigma_\tau^2)}}{\alpha_R \sigma_\tau \{ \coth(\alpha_R N/2) - \operatorname{erf}[\tau/(\sqrt{2}\sigma_\tau)] \}}, \quad (3.25)$$

where

$$\sigma_\tau = \frac{|\eta| \sigma_E}{\beta^2 \omega_{s0} E_0}, \quad \alpha_R = \frac{e^2 \beta^2 E_0 R_s}{\eta T_0 \sigma_E^2}, \quad (3.26)$$

and

$$\operatorname{erf}(x) = \frac{2}{\sqrt{\pi}} \int_0^x e^{-t^2} dt \quad (3.27)$$

is the error function. For a weak beam with $|\alpha_R|N \lesssim 1$, the peak beam density occurs at

$$\tau = \frac{\alpha_R N}{\sqrt{2\pi}} \sigma_\tau. \quad (3.28)$$

This peak moves forward above transition ($\alpha_R > 0$) and backward below transition ($\alpha_R < 0$) as the beam intensity increases. This effect comes from the parasitic loss of the beam particle which is largest at the peak of the linear density $\rho(\tau)$ and smallest at the two ends. Those particles losing energy will arrive earlier/later than the synchronous particle in time above/below transition and the distribution will therefore lean forward/backward. Such bunch profiles are plotted in Fig. 3.2 for $\alpha_R N = -10, -5, 0$,

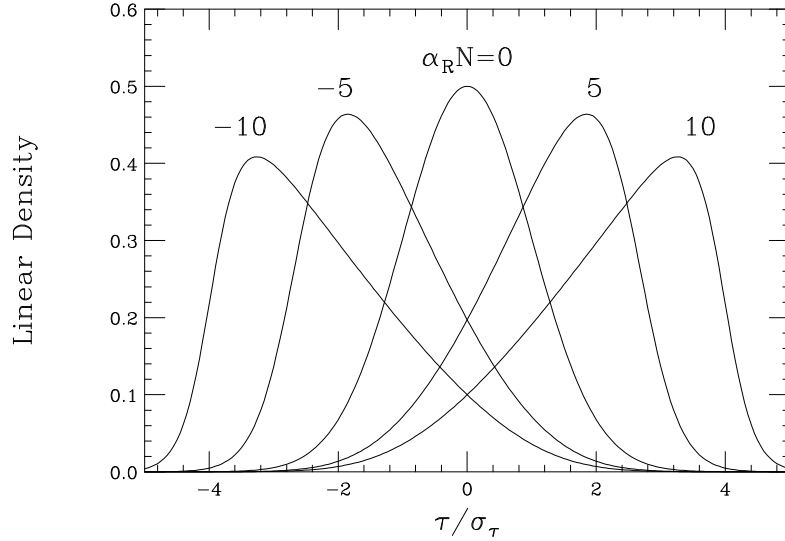


Figure 3.2: Plot of bunch profiles between $\pm 5 \sigma_s$ for $\alpha_R N = -10, -5, 0, 5,$ and 10 , according to the solution of the Haissinski equation when the impedance is purely resistive. These profiles are normalized to $\sigma_\tau \sqrt{\pi/2}$ when integrated over τ . It is evident that the profile leans forward above transition ($\alpha_R > 0$) and backward below transition ($\alpha_R < 0$).

5, and 10. In the plots, the linear densities are normalized to $\sigma_\tau \sqrt{\pi/2}$ when integrated over τ .

When the longitudinal impedance is purely inductive, $W'_0(z) = L\delta'(z/v)$, the double integrals can be performed and the Haissinski equation becomes

$$\rho(\tau) = k e^{-\tau^2/(2\sigma_\tau^2) - \alpha_L \rho(\tau)}, \quad (3.29)$$

where k is a positive constant and $\alpha_L = e^2 \beta^2 E_0 L / (\eta T_0 \sigma_E^2)$. The above can be rewritten as

$$\rho(\tau) e^{\alpha_L \rho(\tau)} = k e^{-\tau^2/(2\sigma_\tau^2)}. \quad (3.30)$$

The right side is an even function of τ and so must be the left side, $\rho e^{\alpha_L \rho}$. Thus, it appears that the distorted distribution ρ is also an even function of τ . The linear distribution will remain left-right symmetric. Thus, the reactive part of the impedance will either lengthen or shorten the bunch, while the resistive part will cause the bunch to lean forward or backward. When $|\alpha_L| N \lesssim 1$, we can iterate,

$$\rho \approx k e^{-\tau^2/(2\sigma_\tau^2)} \left(1 - k \alpha_L e^{-\tau^2/(2\sigma_\tau^2)} \right). \quad (3.31)$$

Without the impedance term, k in Eq. (3.29) represents the particle density at the center of the bunch. Now for $\alpha_L > 0$, Eq. (3.31) says that effectively k becomes smaller. In other words, the distribution spreads out, or the effective rms bunch length becomes larger than σ_τ . This is the situation of either a repulsive inductive impedance force above transition or a repulsive capacitive force ($L < 0$) below transition. On the other hand, for an attractive inductive force below transition or an attractive capacitive force above transition, $\alpha_L < 0$. The bunch will be shortened.

For a general wake function, the Haissinski equation can only be solved numerically. The equation, however, can be cast into the more convenient form (Exercise 3.2)

$$\rho(\tau) = \xi \exp \left[- \left(\frac{\omega_{s0} \beta^2 E_0}{\eta \sigma_E} \right)^2 \frac{\tau^2}{2} - \frac{e^2 \beta^2 E_0}{\eta T_0 \sigma_E^2} \int_0^\infty d\tau' \rho(\tau + \tau') \int_0^{\tau'} d\tau'' W_0'(\tau'') \right]. \quad (3.32)$$

Notice that $\rho(\tau)$ on the left side only depends on the ρ on the right side evaluated in front of τ . We can therefore solve for ρ at successive slices of the bunch by assigning zero or some arbitrary value to ρ at the very first slice (the head) and some value to the constant ξ . The value of ξ is varied until the proper normalization of ρ is obtained.

The longitudinal wake potential of the damping rings at the SLAC Linear Collider (SLC) has been calculated carefully. Using it as input, the Haissinski equation is solved numerically at various beam intensities. The results are shown as solid curves in Fig. 3.3 along with the actual measurements. The agreement has been very satisfactory [2].

3.4 Elliptical Phase-Space Distribution

An easier way to compute the bunch length distorted by the reactive impedance is to consider the elliptical phase-space distribution

$$\psi(\tau, \Delta E) = \frac{3N|\eta|\sqrt{\kappa}}{2\pi\beta^2\omega_{s0}E_0\hat{\tau}_0^3} \sqrt{\hat{\tau}_0^2 - \left(\frac{\eta}{\beta^2\omega_{s0}E_0} \right)^2 \Delta E^2 - \kappa\tau^2} \quad (3.33)$$

for an electron bunch, where $\hat{\tau}_0$ is the unperturbed half bunch length (in time advance). The distribution vanishes when the expression inside the square root of Eq. (3.33) becomes negative. The maximum half energy spread $\widehat{\Delta E}$ derived from Eq. (3.33),

$$\widehat{\Delta E} = \frac{\beta^2\omega_{s0}E_0\hat{\tau}_0}{|\eta|}, \quad (3.34)$$

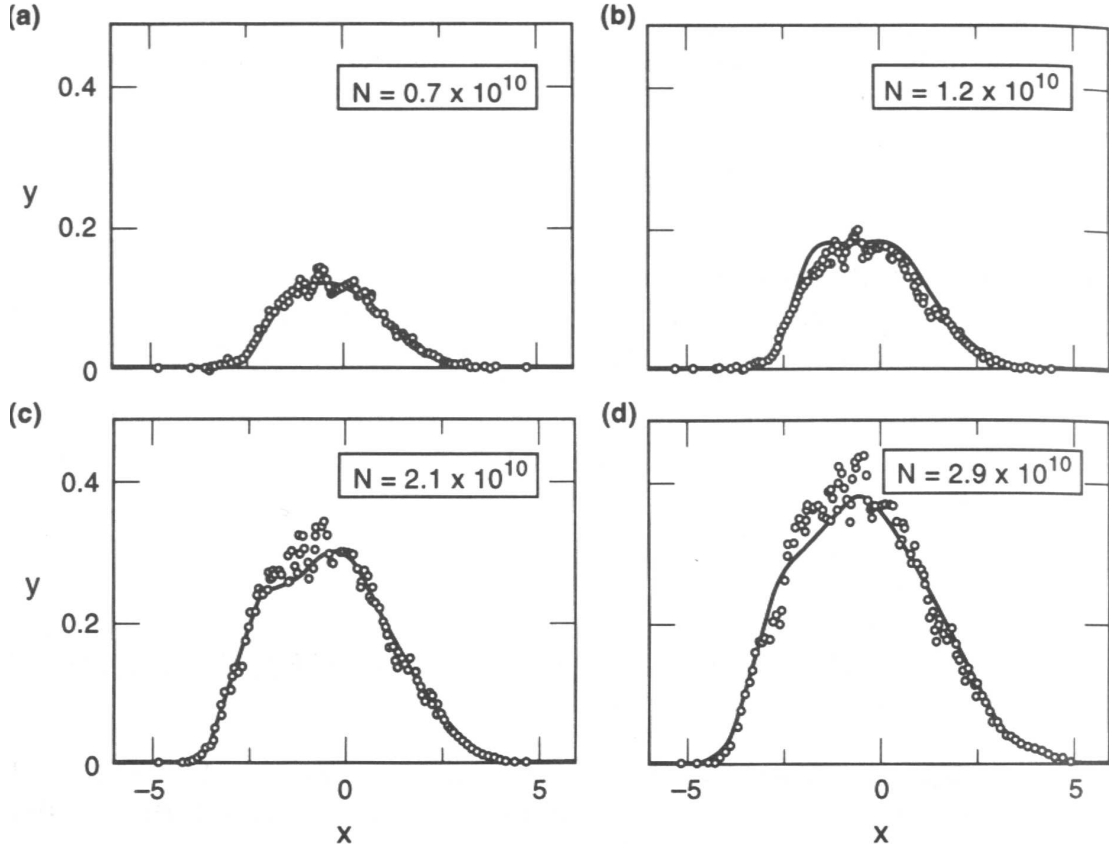


Figure 3.3: Potential-well distortion of bunch shape for various beam intensities for the SLAC SLC damping ring. Solid curves are solution of the Haissinski equation and open circles are measurements. The horizontal axis is in units of unperturbed rms bunch length σ_{z0} , while the vertical scale gives $y = 4\pi e\rho(z)/[V_{rf}'(0)\sigma_{z0}]$. The beam is going to the left.

is exactly that given by the phase equation (2.11). The maximum half energy spread is a constant determined by synchrotron radiation, while the half width of the bunch derived from Eq. (3.33),

$$\hat{\tau} = \frac{\hat{\tau}_0}{\sqrt{\kappa}} \quad (3.35)$$

is determined by the parameter κ . This distribution when integrated over ΔE gives the normalized parabolic linear distribution

$$\rho(\tau) = \frac{3N\sqrt{\kappa}}{4\hat{\tau}_0^3} (\hat{\tau}_0^2 - \kappa\tau^2) . \quad (3.36)$$

With the reactive wake function $W'_0(z) = L\delta'(z/v)$, the Hamiltonian of Eq. (2.20) can therefore be written as a quadratic in ΔE and τ :

$$H = -\frac{\eta}{2v\beta^2 E_0}(\Delta E)^2 - \frac{\omega_{s0}^2 \beta^2 E_0}{2\eta v} \tau^2 - \frac{e^2 L}{C_0} \rho(\tau) . \quad (3.37)$$

Substituting for the linear density $\rho(\tau)$, the Hamiltonian becomes

$$H = \frac{\omega_{s0}^2 \beta^2 E_0}{2\eta v} \left[-\left(\frac{\eta}{\beta^2 \omega_{s0} E_0} \right)^2 \Delta E^2 - \tau^2 (1 - D\kappa^{3/2}) \right] , \quad (3.38)$$

where

$$D = \frac{3e^2 N \eta v L}{2\omega_{s0}^2 \beta^2 E_0 C_0 \hat{\tau}_0^3} , \quad (3.39)$$

and the constant term involving $\hat{\tau}_0$ has been dropped. To be self-consistent, the expression of ψ in Eq. (3.33) must be a function of the Hamiltonian. Comparing Eq. (3.33) with Eq. (3.38), we arrive at

$$\kappa = 1 - D\kappa^{3/2} \quad (3.40)$$

or

$$\left(\frac{\hat{\tau}}{\hat{\tau}_0} \right)^3 = \left(\frac{\hat{\tau}}{\hat{\tau}_0} \right) + D . \quad (3.41)$$

This cubic can be solved by iteration. First we put $\hat{\tau}/\hat{\tau}_0 = 1$ on the right side. If $D > 0$, we find $\hat{\tau}/\hat{\tau}_0 > 1$ or the bunch is lengthened. If $D < 0$, it is shortened. The former corresponds to either an inductive force above transition or a capacitive force below transition. The latter corresponds to either an inductive force below transition or a capacitive force above transition. This is illustrated in the first row of Fig. 3.4, where we notice that the energy spread of the bunch is unchanged for various types of perturbation.

For a proton bunch, the energy spread is also modified but the bunch area remains constant. The phase-space distribution has to be rewritten as

$$\psi(\tau, \Delta E) = \frac{3N|\eta|}{2\pi\beta^2\omega_{s0}E_0\hat{\tau}_0^3} \sqrt{\hat{\tau}_0^2 - \frac{1}{\kappa} \left(\frac{\eta}{\beta^2\omega_{s0}E_0} \right)^2 \Delta E^2 - \kappa\tau^2} . \quad (3.42)$$

Now we have (Exercise 3.6)

$$\hat{\tau} = \frac{\hat{\tau}_0}{\sqrt{\kappa}} \quad \text{and} \quad \widehat{\Delta E} = \sqrt{\kappa} \widehat{\Delta E}_0 . \quad (3.43)$$

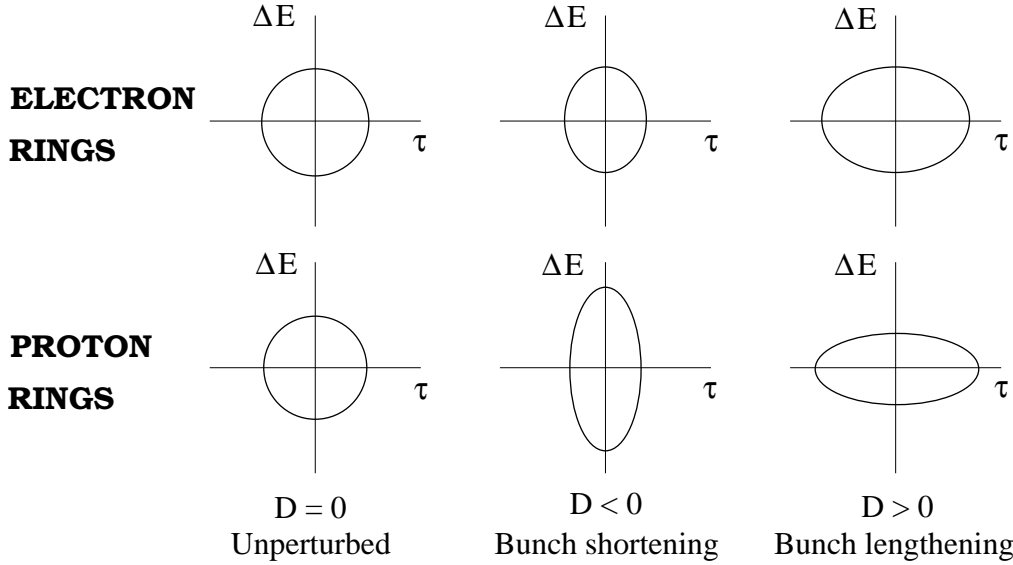


Figure 3.4: Potential well distortion of the bunch shape in the longitudinal phase space. $D > 0$ corresponds to either an inductive perturbation above transition or a capacitive perturbation below transition, while $D < 0$ implies either an inductive perturbation below transition or a capacitive perturbation above transition. Top row is for electron rings where the energy spread remains constant as a result of radiation damping. Bottom row is for proton rings where the bunch area is constant.

Again comparing with the Hamiltonian, we arrive at the quartic equation

$$\left(\frac{\hat{\tau}}{\hat{\tau}_0}\right)^4 = 1 + D \left(\frac{\hat{\tau}}{\hat{\tau}_0}\right). \quad (3.44)$$

This is illustrated in the bottom row of Fig. 3.4.

3.5 Synchrotron Tune Shift

When the potential well is distorted, the frequency of oscillation will be changed also. For an elliptical bunch distribution in the longitudinal phase space, the synchrotron oscillation frequency shift can be easily extracted from the Hamiltonian in Eq. (3.38). We get

$$\left(\frac{\omega_s}{\omega_{s0}}\right)^2 = \left(1 + \frac{\Delta\omega_s}{\omega_{s0}}\right)^2 = 1 - D\kappa^{3/2}. \quad (3.45)$$

As a first approximation, the synchrotron frequency shift $\Delta\omega_s$ or synchrotron tune shift $\Delta\nu_s$ is given by

$$\frac{\Delta\omega_s}{\omega_{s0}} = \frac{\Delta\nu_s}{\nu_{s0}} \approx -\frac{D}{2} = -\frac{3e^2 N \eta v L}{4\omega_{s0}^2 \beta^2 E_0 C_0 \hat{\tau}_0^3}, \quad (3.46)$$

where $\omega_{s0}/(2\pi)$ is the *bare* or *unperturbed* synchrotron frequency and $\nu_{s0} = \omega_{s0}/\omega_0$ is the *bare* or *unperturbed* synchrotron tune. We see that an inductive vacuum chamber will lower/increase the synchrotron tune above/below transition. For the longitudinal space charge self-force, the synchrotron tune will be shifted upward/downward above/below transition. Notice that this is the tune shift for an individual particle and is called the *incoherent* tune shift.

For a more general bunch distribution and a more general impedance, we resort to the equations of motion [Eqs. (2.11) and (2.12)], from which we obtain

$$\frac{d^2\tau}{ds^2} + \frac{\nu_{s0}^2}{R^2} \tau = -\frac{\eta}{v\beta^2 E_0} \left[\langle F_0^{\parallel}(\tau, s) \rangle - \langle F_0^{\parallel}(0, s) \rangle \right]. \quad (3.47)$$

The wake force on the right side is

$$\langle F_0^{\parallel}(\tau, s) \rangle - \langle F_0^{\parallel}(0, s) \rangle = -\frac{e^2}{C_0} \int_{-\infty}^{\infty} d\tau' \rho(\tau', s) \left[W_0'(\tau' - \tau) - W_0'(\tau') \right]. \quad (3.48)$$

To obtain the synchrotron tune shift in the dipole mode, we linearize the wake force, or

$$\langle F_0^{\parallel}(\tau, s) \rangle - \langle F_0^{\parallel}(0, s) \rangle = \left[\frac{e^2}{C_0} \int_{-\infty}^{\infty} d\tau' \rho(\tau', s) W_0''(\tau') \right] \tau. \quad (3.49)$$

The synchrotron tune shift can therefore be read out easily as

$$\frac{\Delta\nu_s}{\nu_{s0}} = \frac{e^2 \eta R}{4\pi \nu_{s0}^2 v \beta^2 E_0} \int_{-\infty}^{\infty} d\tau' \rho(\tau', s) W_0''(\tau'). \quad (3.50)$$

As a check, let us substitute for the inductive wake potential $W_0'(\tau) = L\delta'(\tau)$. The integral can be performed to get

$$\frac{\Delta\nu_s}{\nu_{s0}} = \frac{e^2 \eta R L}{4\pi \nu_{s0}^2 v \beta^2 E_0} \left. \frac{\partial^2 \rho}{\partial \tau^2} \right|_{\tau=0}. \quad (3.51)$$

If we substitute for the parabolic bunch distribution of Eq. (3.36), we get back the tune shift result obtained in Eq. (3.46).

If we average Eq. (3.47) over all the beam particles, we obtain the equation of motion of the center-of-mass of the bunch and we can compute the *coherent* synchrotron tune

shift of the bunch due to potential-well distortion. However, there is another contribution to this coherent tune shift from the dynamic part of the perturbation which we are going into later (see Sec. 9.1.1 below). This dynamic contribution will cancel the potential-well contribution, resulting in no coherent synchrotron tune shift in the dipole mode when the bunch intensity is weak and the wake is no longer than the bunch spacing. Physically, this dipole mode is a rigid rotation of the bunch in the longitudinal phase space. The wake field pattern, and therefore the potential-well distortion, moves with the bunch. Thus, the motion of the bunch as a whole is not affected by the wake field at all. On the other hand, the picture for incoherent motion is about a beam particle moving inside the bunch with the bunch center at rest. An individual particle can therefore sample a variation of the wake field while executing synchrotron oscillation. Thus, to demonstrate the effect of space charge impedance or inductive impedance, the coherent quadrupole mode of the synchrotron oscillation should be measured. If the incoherent synchrotron tune is desired, a Schottky scan of the beam is necessary.

3.6 Potential-Well Distortion Compensation

Potential-well distortion can often be a serious problem in the operation of an accelerator or storage ring. If the distortion opposes the rf bunching, a much larger rf voltage and hence rf power will be required to counteract the distortion. Even when such a higher compensating rf voltage is available, the rf bucket may have been so much distorted that its useful area has very much been reduced. An example is the Los Alamos Proton Storage Ring (PSR), which stores an intense proton beam at the kinetic energy of 797 MeV. The ring has a transition gamma of $\gamma_t = 3.1$, implying that the operation of the ring is below transition. The longitudinal space charge force is therefore repulsive in nature and tends to lengthen the bunch. This longitudinal repulsive force will counteract the rf bunching force. We will study how serious the potential-well distortion is and a possible way to cure the problem.

The PSR has a circumference of 90.2 m. It receives chopped proton beams from a linac cumulatively in 1000 to 2000 turns. The beam is bunched by an rf buncher to the desired length and is then extracted for experimental use. The rf buncher is of rf harmonic $h = 1$, or there is only one bunch. The revolution frequency and the rf frequency are both 2.796 MHz. A typical store consists of a bunch consisting of 3.2×10^{13} protons, of half length $\hat{\tau} = 133.5$ ns, occupying roughly two third of ring, and a half

energy spread of $\widehat{\Delta E}/E_0 = 0.005$. If space charge is neglected, to keep such a bunch matched to the rf bucket, the synchrotron tune is

$$\nu_{s0} = \frac{|\eta|\widehat{\Delta E}_0}{\omega_0\beta^2 E_0\hat{\tau}} = 0.000402 , \quad (3.52)$$

and the required rf voltage is

$$V_{\text{rf}} = \frac{2\pi\beta^2 E_0\nu_{s0}^2}{e|\eta|h} = 6.60 \text{ kV} . \quad (3.53)$$

Now let us estimate the space charge effect [4]. The 95% (or full) normalized transverse emittance is $50 \times 10^{-6} \text{ } \pi\text{m}$. From this and the ring lattice, the g_0 factor has been estimated to be

$$g_0 = 1 + 2 \ln \frac{b}{a} \approx 3.0 , \quad (3.54)$$

where a is the beam radius and b is the beam pipe radius. The longitudinal space charge impedance is therefore

$$\left(\frac{Z_0^{\parallel}}{n} \right)_{\text{spch}} = i \frac{Z_0 g_0}{2\gamma^2\beta} \approx i196 \text{ } \Omega . \quad (3.55)$$

According to Eq. (3.19), a particle with an arrival time τ ahead of the synchronous particle sees an electric field

$$E_{s\text{spch}} = -\frac{e}{2\pi\beta c} \left| \frac{Z_0^{\parallel}}{n} \right|_{\text{spch}} \frac{d\lambda}{d\tau} , \quad (3.56)$$

where $\lambda(\tau)$ is the linear particle density of the bunch and is normalized to the number of particles in the bunch by integrating over τ . This electric field comes from the longitudinal space charge effect and is in the direction of the motion of the bunch. It is positive in the head half of the bunch ($\tau > 0$) and negative in the tail half ($\tau < 0$). It is therefore repulsive. Assume a parabolic distribution,

$$\lambda(\tau) = \frac{3N}{4\hat{\tau}} \left(1 - \frac{\tau^2}{\hat{\tau}^2} \right) , \quad (3.57)$$

so that the electric field becomes linear in τ . The particle will gain in a turn the potential

$$V_{\text{spch}} = E_{s\text{spch}} C_0 = \frac{3eN}{2\omega_0\hat{\tau}^2} \left| \frac{Z_0^{\parallel}}{n} \right|_{\text{spch}} \frac{\tau}{\hat{\tau}} = 4.82 \frac{\tau}{\hat{\tau}} \text{ kV} , \quad (3.58)$$

according to its position in the bunch. This potential is of roughly the same size as the rf voltage required if there is no space charge. Thus, in the presence of space charge, we need to increase V_{rf} from 6.60 kV to approximately $6.60 + 4.82 = 11.42$ kV; nearly 42% of the rf voltage has been spent to counteract the space charge force. One must realize that the rf buncher at PSR was capable to deliver only 12 kV in 1997. Although the rf buncher has been upgraded to about 18 kV, there is also a goal to increase the beam intensity to 5×10^{13} protons as well. It is important to point out that rf compensation to space charge can never be exact. The rf force is sinusoidal while the space charge force is linear if the linear distribution is parabolic. Although the space charge force may become sinusoidal-like if the unperturbed linear beam distribution is Gaussian, the frequency content is still very different from the rf focusing force.

3.6.1 Ferrite Insertion

It has been proposed that if ferrite rings (also called cores) are installed inside the vacuum chamber, the proton beam will see an extra inductive impedance from the ferrite, and hopefully this inductive impedance will cancel the capacitive space charge impedance of the beam [5, 6]. Toshiba M_4C_{21A} ferrite rings are used, each having an inside diameter $d_i = 12.7$ cm, outside diameter $d_o = 20.3$ cm, and thickness $t = 2.54$ cm. The relative magnetic permeability is $\mu' \approx 70$ at the PSR rotation frequency, 2.796 MHz. With n_f ferrite rings stacked together, the impedance per harmonic is

$$\frac{Z_0^{\parallel}}{n_{\text{ferrite}}} = -i \frac{Z_0 \omega_0 t n_f}{2\pi c} \mu' \ln \frac{d_o}{d_i} = 2.93 n_f \Omega . \quad (3.59)$$

Thus, to cancel a space charge impedance per harmonic of $\sim 300 \Omega$, about $n_f = 102$ will be needed. Three ferrite inserts were assembled. Each consisted of a stainless-steel pill-box cavity having an inner diameter of 20.3 cm and inner length of 75.5 cm, so that 30 ferrite cores could be packed inside. To prevent charge buildup on the inner surface of the cores, each of the cores were treated with a very thin ($1 \text{ M}\Omega$ per square) conductive coating (Heraeus R8261) baked on the inner and outer surface. Additional radial conducting ‘spokes’ were added to provide conductivity from the inner surface to the outer wall of the chamber. Solenoidal wiring was wound outside the stainless steel container so that the magnetic permeability of the ferrite could be controlled.

Two such ferrite tuners or inserts were installed in the PSR in 1997. To study space charge compensation caused by the installed inductance, two experiments, using different

bunch lengths, were completed. The designated charge configurations were injected into the PSR and the longitudinal profiles (bunch length and shape) were observed, digitized, and recorded using signals from a wide-band wall current monitor at the end of each 625- μ s injection period. The experiments were performed for two bunch lengths: ~ 50 ns (half length) with 4.0×10^{12} particles and ~ 150 ns (half length) with 1.2×10^{13} . The rf voltage was set to 7 kV in both cases. The resulting waveforms are compared with detailed particle tracking simulations in Fig. 3.5 for the two bunch lengths. The solid curve in the top left plot represents the bunch shape with the full effect of the inserted inductance (zero bias). The dotted curve corresponds to data with the effect of the inductance diminished by 900-A dc bias. The difference of peak heights is about 16%. Simulations performed with assumed injection momentum spread $\Delta p/p = 0.08\%$ are shown in the top right plot. They predict an rms bunch length of 19 ns, but increasing to 22 ns when the ferrite bias current is raised to 900 A with the inductance reduced to 34% of its unbiased value. We see that the experiment measurements are consistent with the simulation predictions. Similar conclusion can be drawn for the long-bunch-length situation shown in bottom plots of Fig. 3.5. We see that bunch lengths have been reduced with the ferrite insertion, indicating that the space charge impedance has been cancelled to a certain extent.

It is unfortunate that the change in synchrotron frequency could not be measured to give another demonstration of the cancellation of space charge. This is mainly due to the slow synchrotron oscillation in the PSR. During the whole accumulation and storage time, the beam particles usually make less than one synchrotron oscillation. A similar space charge compensation experiment had also been performed at the KEK PS Main Ring, but with a much lower intensity of 2 to 9×10^{11} protons per bunch [7]. The beam kinetic energy was 500 MeV with a space charge impedance $Z_0^{\parallel}/n = i310 \Omega$. Instead of ferrite, the inductor inserts or tuners were loaded with a Met-Glass-like material called Finemet. Since the coherent synchrotron frequency in the dipole mode is not affected by space charge, the coherent frequency of the quadrupole synchrotron oscillation was measured instead as a function of bunch intensity. The inductor tuners were not equipped with biased current coil to control the permeability of the Finemet. In order to alleviate the effect of the Finemet when required, mechanical copper shorts were installed across the inductor tuners instead. As shown in Fig. 3.6, with several inductor tuners installed, the coherent frequency was less dependent on intensity without the mechanical shorts than with the mechanical shorts, indicating that the space charge force had been partially cancelled by the Finemet cores.

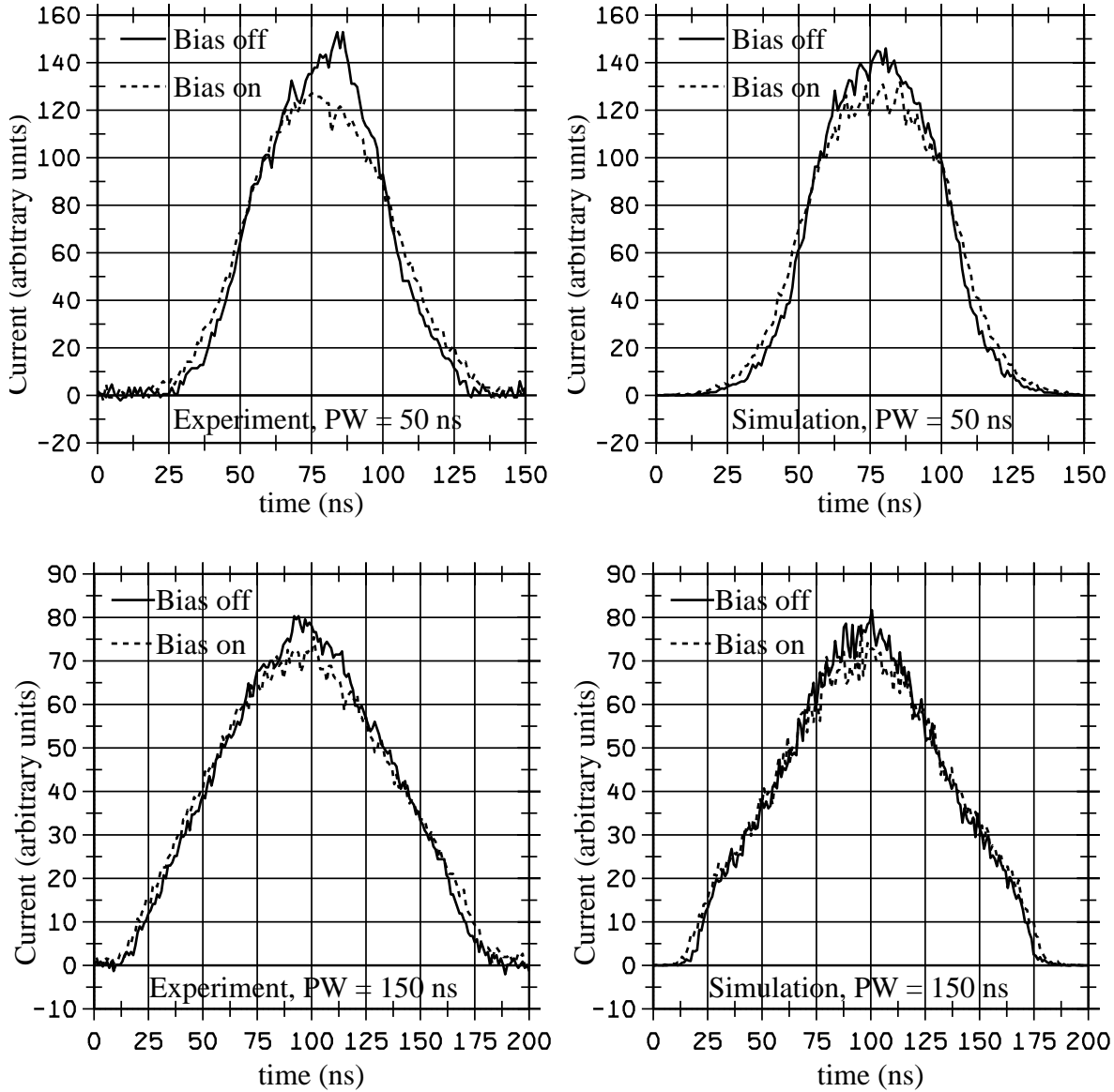


Figure 3.5: Measured (left) and simulated (right) pulse shapes after $625 \mu\text{s}$, for injected pattern widths of 50 ns with 4.0×10^{12} protons (bottom) and 150 ns with 1.2×10^{13} protons. In both cases, $V_{\text{rf}} = 7.5 \text{ kV}$. Solid: no bias, dotted: 900-A bias or a reduction of μ' by factor of 34%.

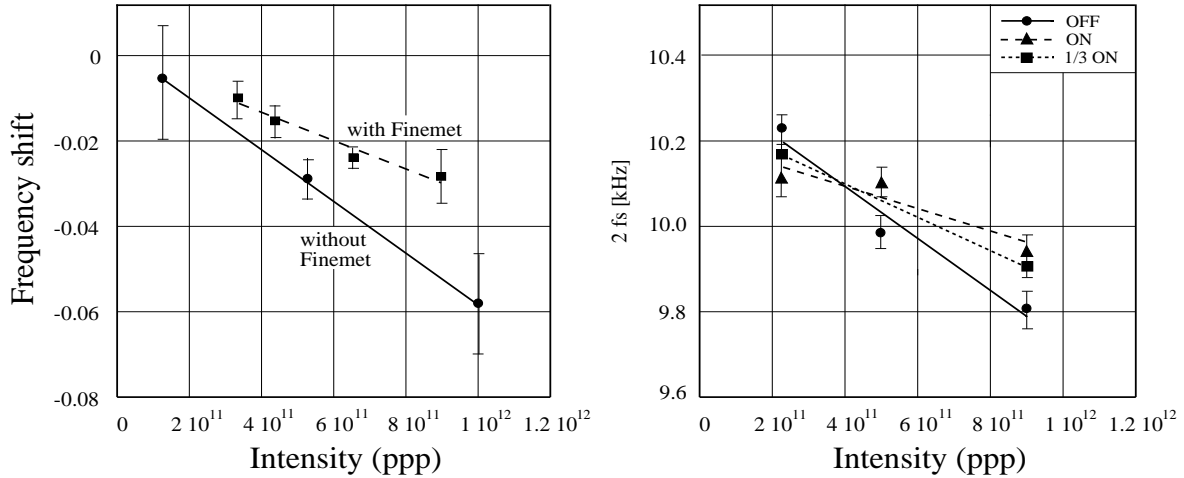


Figure 3.6: Left: Measured frequency shifts of the quadrupole oscillations versus beam intensity at KEK with and without Finemet insertion. Right: New KEK results of quadrupole oscillation frequency versus beam intensity with Finemet tuners on, $\frac{1}{3}$ on, and off.

The second experiment at the PSR is to measure the onset of vertical instability using a short-stripline beam-position monitor. With a 3.0×10^{13} proton beam stored, the rf voltage was lowered until vertical instability was registered. This signal comes about when the rf bucket is not large enough to hold the bunch so that some protons spill out into the bunch gap. These protons in the gap trap electrons preventing them to be cleared and causing a transverse e-p instability. Many previous performance points (blue squares) are plotted in Fig. 3.7 as the required buncher voltage versus beam intensity. The historical performance is roughly represented by the dashed line. The results of this experiment are indicated by red triangles. It was found that less buncher voltage was required to sustain the beam in the presence of the inductor inserts. For example, at the highest intensity that could be reached during the experiment, 3×10^{10} protons in the beam, only 6.9 kV was required, which amounted to a $\sim 60\%$ reduction of what had previously been necessary to maintain stability. This result indicates that the space charge impedance has been compensated to a certain extent by the ferrite cores installed in the vacuum chamber. Thus, less rf voltage will be required to bunch the proton beam. At the same time, it was found that the bunch gap was the cleanest ever observed.

This experiment, however, has far from being perfect. First, there are only a few points measured (the red triangles in Fig. 3.7); the indication is therefore not very convincing. Second, the bunch lengthening when the solenoidal bias was turned on had

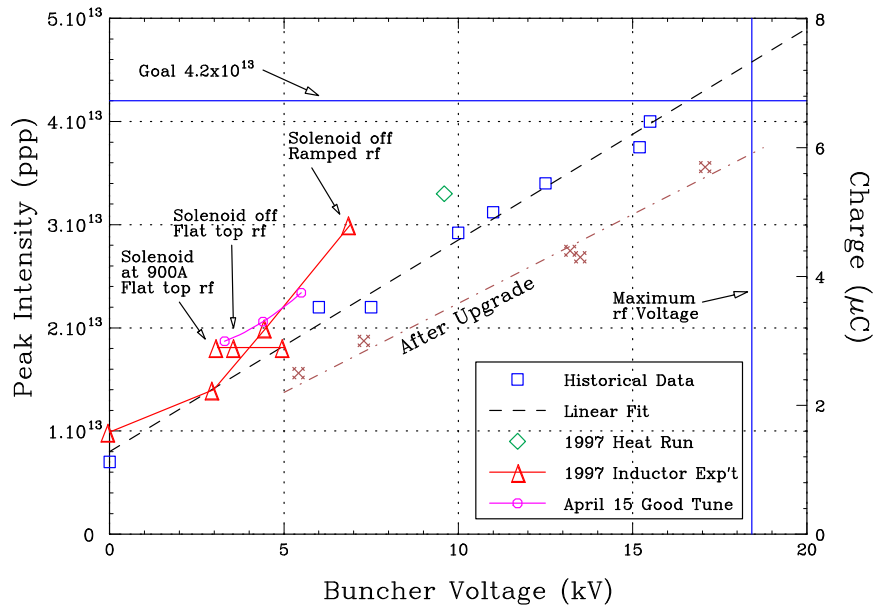


Figure 3.7: The performance of the PSR: the required buncher voltage plotted against the intensity of the beam. The dashed line shows roughly the historical performance before upgrade. The red triangles are results of the experiment discussed here. For example, with the ferrite insertion without solenoidal bias, only 6.9 kV is required to hold a bunch containing 3×10^{13} protons, which is about $\frac{1}{3}$ less than the historical value.

only been minimal and not spectacular (see Fig. 3.5), leaving behind the question of the efficiency about the inserts—how much space charge had actually been compensated. Third and worst of all, a longitudinal instability had been observed, although at the intensity of 3.2×10^{13} protons, this instability had been small and appeared to be tolerable. Because of these and other reasons, the ferrite inserts were removed during the upgrade. After the upgrade, when the machine was turned on, however, the performance was very poor as is indicated by the dot-dashed line in Fig. 3.7. In order to improve the performance, the inductor inserts were once again installed. But with the upgraded beam intensity, the small longitudinal instability had become so intense that the beam profiles became heavily distorted and there was a considerable of beam loss. This instability together with its eventual cure will be discussed in detail in Sec. 6.3.

3.7 Exercises

- 3.1. Show that the geometric factor defined Eq. (3.10) for the longitudinal space charge impedance becomes

$$g_0 = \frac{1}{2} + 2 \ln \frac{b}{a}, \quad (3.60)$$

when the longitudinal electric field opposing the beam is averaged over all the beam particles. In above, b is the radius of the beam pipe and a is the transverse radius of the beam.

- 3.2. Transform the Haissinski equation (3.23) according to the following:

- (1) Notice that the integral over τ'' can be rewritten as

$$\int_0^\tau d\tau'' \rightarrow - \int_\tau^\infty d\tau'' + \text{constant}, \quad (3.61)$$

where the constant can be absorbed into the normalization constant $\rho(0)$ which we rename by ξ .

- (2) The integration in the τ' - τ'' space is in the 0° to 45° quadrant between the lines $\tau'' = \tau$ and $\tau'' = \tau'$. Translate the τ' and τ'' axes so that the region of integration is now between the τ' -axis and the 45° line $\tau'' = \tau'$.

- (3) Integrate over τ'' first from 0 to τ' ; then integrate over τ' .

- (4) Change the variable τ'' to $\tau' - \tau''$. Now the Haissinski equation takes the more convenient form of Eq. (3.32), or

$$\rho(\tau) = \xi \exp \left[- \left(\frac{\omega_{s0} \beta^2 E_0}{\eta \sigma_E} \right)^2 \frac{\tau^2}{2} - \frac{e^2 \beta^2 E_0}{\eta T_0 \sigma_E^2} \int_0^\infty d\tau' \rho(\tau + \tau') \int_0^{\tau'} d\tau'' W'_0(\tau'') \right]. \quad (3.62)$$

- 3.3. The bunch in the Fermilab Tevatron contains $N = 2.7 \times 10^{11}$ protons and has a designed half length of $\hat{\tau} = 2.75$ ns. The ring main radius is $R = 1$ km and the slip factor is $\eta = 0.0028$ at the incident energy of $E_0 = 150$ GeV. The rf harmonic is $h = 1113$ and the rf voltage is $V_{\text{rf}} = 1.0$ MV. Assume a broadband impedance centered at $\omega_r/(2\pi) \approx 3$ GHz, quality factor $Q = 1$, and shunt impedance $R_s = 250$ k Ω .

- (1) Show that the frequencies that the bunch samples are much less than the resonant frequency of the broadband, so that the asymmetric beam distortion driven by $\text{Re} Z_0^\parallel$ can be neglected.

(2) Using only the inductive part of the impedance at low frequencies, compute from Eq. (3.44) the equilibrium bunch length as a result of potential-well distortion.

(3) Electron bunches are usually very short. If an electron bunch of rms bunch length 2 cm is put into the Tevatron, show that its spectrum will sample the resonant peak of $\mathcal{R}e Z_0^{\parallel}$ and may suffer asymmetric distortion. Compute the asymmetric factor $\alpha_R N$ given by Eq. (3.25) and determine whether the asymmetry is large or not.

3.4. From Eq. (3.41) for an electron bunch, show that there are two solutions for the perturbed bunch length due to distortion by a capacitive impedance when $-2/3^{3/2} < D < 0$. Which one is physical? When $D < -2/3^{3/2}$, there is no solution. At this critical situation, the bunch shortening ratio is $3^{-1/2}$.

Hint: Transform Eq. (3.41) to

$$4x^3 - 3x = \frac{3^{3/2}}{2}D \quad (3.63)$$

and substitute for $x = \sin \theta$. What is the right side in terms of θ ?

3.5. When the coupling impedance is purely resistive,

(1) derive the potential-well distorted linear distribution, Eq. (3.25).

(2) Show that when the intensity of the bunch is weak, the peak of the distribution is given by Eq. (3.28).

Hint: Transform the Haissinski equation to a differential equation,

$$\rho' + \frac{\tau}{\sigma_\tau^2} \rho - \alpha_R \rho^2 = 0 . \quad (3.64)$$

Solve the equation and determine $\rho(0)$.

3.6. Starting from Eq. (3.42), filling in the missing steps, derive the quartic equation (3.44) for the proton half bunch length under the influence of a purely reactive longitudinal impedance.

Bibliography

- [1] J. Haissinski, *Nuovo Cimento* **18B**, 72 (1973).
- [2] K.L.F. Bane and R.D. Ruth, *Proc. IEEE Conf. Part. Accel.*, Chicago, 1989, p.789.
- [3] A.G. Ruggiero, *IEEE Trans. Nucl. Sci.* **NS-24**, 1205 (1977).
- [4] K.Y. Ng and Z. Qian, *Instabilities and Space-Charge Effects of the High-Intensity Proton Driver*, Fermilab Report FN-659, 1997, AIP Conference Proceedings 435, Workshop on Physics at the First Muon Collider and at the Front End of the Muon Collider, Ed. S. Geer and R. Raja, Batavia, IL, Nov. 6-9, 1997, p. 841.
- [5] J.E. Griffin, K.Y. Ng, Z.B. Qian, and D. Wildman, Fermilab Report FN-661, 1997.
- [6] Plum, M.A., Fitzgerald, D.H., Langenbrunner, J., Macek, R.J., Merrill, F.E., Neri, F., Thiessen, H.A., Walstrom, P.L., Griffin, J.E., Ng, K.Y., Qian, Z.B., Wildman, D., and Prichard, B.A. Jr., *Phys. Rev. ST Accel. Beams*, **2**, 064201 (1999).
- [7] Koba, K., Machida, S., and Mori, Y., KEK Note, 1997 (unpublished); Koba, K., these proceedings; Koba, K., *et al*, *Phys. Sci. Instr.*, **70**, 2988 (1999).

